A data brief on magnesium isotope compositions of marine calcareous sediments and ferromanganese nodules

Estelle F. Rose-Koga, Francis Albarède

Geochemistry Geophysics Geosystems G3
AN ELECTRONIC JOURNAL OF THE EARTH SCIENCES
Published by AGU and the Geochemical Society

Data Brief
Volume 11, Number 3
11 March 2010
Q03006, doi:10.1029/2009GC002899
ISSN: 1525-2027

A data brief on magnesium isotope compositions of marine calcareous sediments and ferromanganese nodules

Estelle F. Rose-Koga
Laboratoire de Sciences de la Terre, ENS Lyon, 46 allée d'Italie, F-69007 Lyon, France

Now at Laboratoire Magmas et Volcans, Clermont Université, Université Blaise Pascal, BP 10448, F-63000 Clermont-Ferrand, France (e.koga@opgc.univ-bpclermont.fr)

Also at UMR 6524, CNRS, 5 rue Kessler F-63038 Clermont-Ferrand CEDEX, France

Also at IRD, R 163, 5 rue Kessler F-63038 Clermont-Ferrand CEDEX, France

Francis Albarède
Laboratoire de Sciences de la Terre, ENS Lyon, 46 allée d'Italie, F-69007 Lyon, France (francis.albarede@ens-lyon.fr)

[1] The magnesium isotope compositions of 26 ferromanganese nodules from various oceans and 22 calcareous sediment samples from Ocean Drilling Program (ODP) leg sites from the Atlantic (ODP704, leg 114) and the Pacific (ODP846, leg 138) have been analyzed by Multicollector–Inductively Coupled Plasma–Mass Spectrometer. Most nodules from the Pacific and Atlantic oceans have δ^{26}Mg (between -1.89 ± 0.24 and -0.54 ± 0.01‰, 2σ) scatter around the average ocean water value of -0.86 ± 0.12‰. Indian Ocean nodules display a large variation in δ^{26}Mg ranging from -2.94 ± 0.46 to $+0.69 \pm 0.18$‰. As for calcareous sediments, δ^{26}Mg variations range between -2.94 ± 0.50 and -0.71 ± 0.45‰ and between -4.00 ± 0.31 and -1.63 ± 0.09‰ for the Atlantic and the Pacific legs, respectively. This study allows the construction of a thread of global δ^{26}Mg mapping in Fe-Mn nodules and suggests that what controls the δ^{26}Mg variations of marine calcareous sediments is complex and probably linked both to a mixture of different tests of micro-organisms and to diagenesis.

Components: 6620 words, 5 figures, 4 tables.

Keywords: magnesium isotopes; ferromanganese nodules; carbonates; calcareous sediments.

Index Terms: 1050 Geochemistry: Marine geochemistry (4835); 1041 Geochemistry: Stable isotope geochemistry (0454); 4825 Oceanography: Biological and Chemical: Geochemistry.

Received 15 October 2009; **Revised** 20 December 2009; **Accepted** 30 December 2009; **Published** 11 March 2010.

Rose-Koga, E. F., and F. Albarède (2010), A data brief on magnesium isotope compositions of marine calcareous sediments and ferromanganese nodules, *Geochem. Geophys. Geosyst.*, *11*, Q03006, doi:10.1029/2009GC002899.

1. Introduction

[2] Magnesium is a major element in the solid Earth and the second most abundant cation in the oceans behind sodium (1276 ppm and 10764 ppm, respectively [*Edmond et al.*, 1979]). The terrestrial magnesium cycle has been investigated since the sixties [e.g., *Mackenzie and Garrels*, 1966], and the main source of seawater Mg is continental river runoff (5.2×10^{12} mol/yr [*Spencer and Hardie*, 1990; *Wilkinson and Algeo*, 1989]). The two main sinks of Mg are carbonate deposition (0.8×10^{12} mol/yr [*Berner and Berner*, 1996]) and hydrothermal circulation at elevated temperature and in many instances at low temperatures as well (between 0.5×10^{12} and 2×10^{12} mol/yr [*Edmond et al.*, 1979; *Hart and Staudigel*, 1982; *Mottl and Wheat*, 1994; *de Villiers and Nelson*, 1999]). Although much of the river input Mg^{2+} is removed from the oceans by the reaction of seawater with oceanic basalts, it is difficult to assess if really the source and sinks of Mg^{2+} perfectly balance considering the removal rate is still somewhat uncertain. In this case, the long residence time of magnesium (≈13 Myr [e.g., *Broecker and Peng*, 1982]) relative to the ocean mixing time predicts that this dissolved species should be homogenously distributed throughout the oceans (≈1300 ppm). The homogeneous magnesium isotope composition of the oceans, as predicted by the long residence time, has been confirmed independently, and is $\delta^{26}Mg = -0.80 \pm 0.04$ for Atlantic SMOW compared to the DSM3 standard [*Young and Galy*, 2004]. On the other hand the riverine $\delta^{26}Mg$ input to the ocean is not constant and varies depending on the underlying lithologies and on secondary processes during weathering [*de Villiers et al.*, 2005; *Tipper et al.*, 2006a, 2006b, 2008; *Pogge von Strandmann et al.*, 2008; *Brenot et al.*, 2008].

[3] In this study, we investigate and report the magnesium isotope compositions of two different oceanic lithologies: hydrogenous Fe-Mn nodules that are products of both direct and indirect precipitation in the marine environment, therefore potentially possessing a record of the oceanographic conditions under which they have grown, and of marine carbonates from Ocean Drilling Program (ODP) leg 138 (Pacific, 3° south of the Galapagos Islands) and ODP leg 114 (Atlantic) that were selected for their longer time record. We have found $\delta^{26}Mg$ variations in both Fe-Mn nodules and calcareous marine sediments that identify that more than one process fractionates marine magnesium isotopes and that diagenesis is the main process suspected in the case of Fe-Mn nodules.

2. Samples and Methods

2.1. Samples

2.1.1. Manganese Nodules

[4] Fourteen manganese nodules from the Indian Ocean, seven from the Pacific Ocean, one from the Agulhas Basin and four from the Atlantic Ocean were selected to represent the variety of ocean basins and environmental settings (Figure 1). Most of the circum Antarctic samples have already been analyzed for transition elements, Nd, Hf and Pb isotopes [*Albarède et al.*, 1997, 1998; *Abouchami and Goldstein*, 1995] and some of the Indian Ocean samples have already been analyzed for Pb isotopes as well [*Vlastelic et al.*, 2001].

2.1.2. Calcareous Marine Sediments

[5] Cores from ODP leg 138 site 846, hole B (later called ODP 846B) and from leg 114 site 704, hole A (later called ODP 704A) have been used for this study as representative of Pacific and Atlantic Ocean calcareous sediments, respectively. Calcareous sediment samples were obtained from the Lamont-Doherty Core Repository. Sample locations for nodules and the two ODP leg sites are shown in Figure 1.

2.2. Methods

2.2.1. Manganese Nodules

2.2.1.1. Sample Attack

[6] Approximately 20 to 30 mg of samples taken from the nodule surface layer were attacked in a Teflon beaker by a 7:1 mixture of concentrated HF and concentrated HNO_3. The closed beaker was left for more than 8 h on a hot plate (120°C). Subsequent completion of the attack was visually confirmed by the absence of residual particles. After evaporation, the dry residue was dissolved in 6N HCl and the beaker was left closed for another 8 h on a hot plate (120°C). After opening the beaker and when all the solution was evaporated, the dry residue was dissolved in 1 ml of 0.05N HCl. Out of this 1 ml, 100 μl is put aside, dried and redissolved in 10 ml of 2% HNO_3 for chemical analysis (Inductively Coupled Plasma–Mass Spectrometer (ICP-MS) model X7). The remaining 0.9 ml went through Mg chemical separation before Mg isotope analysis.

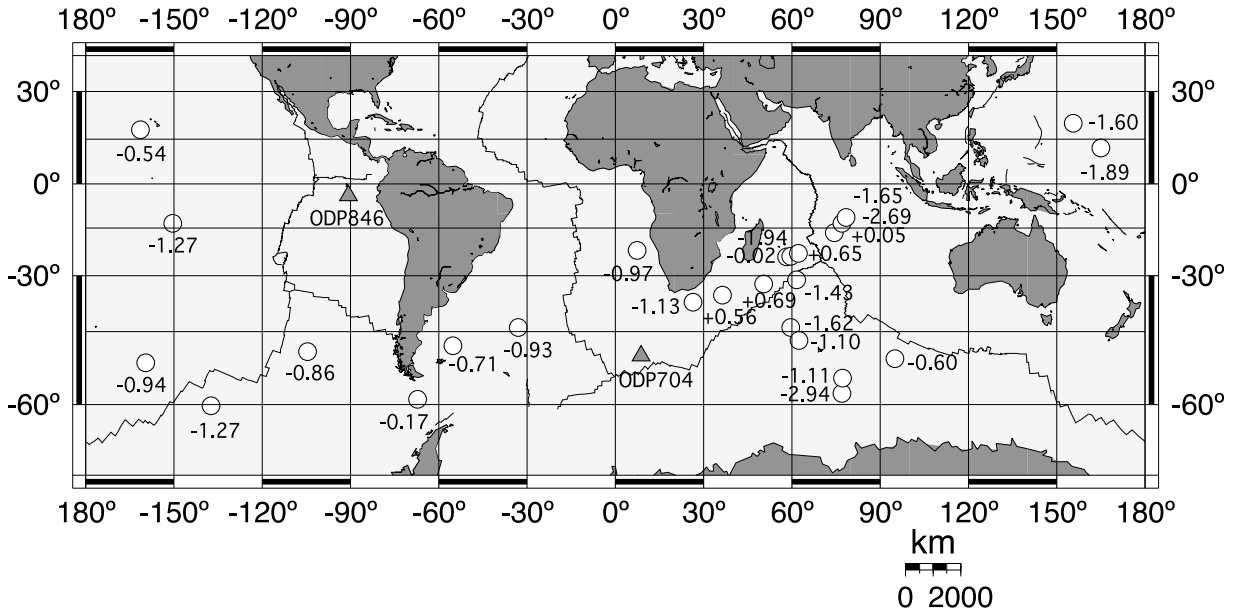

Figure 1. Sampling location for the 26 Fe-Mn nodules (white circles) and the two ODP sites (gray triangles). Beside the white circles are the $\delta^{26}Mg_{DSM3}$ compositions (in ‰) of the surface layers of the Fe-Mn nodules. Samples were collected at depths ranging from 2125 to 5450 m below sea level. Atlantic and Pacific samples are far from any ocean ridge (>800 km). Indian Ocean samples are, in general, located around the Rodriguez triple junction, in the Madagascar basin, in the central Indian basin, and in the Crozet basin except for the two most southern samples (south of 55°S, closer to Antarctica). The two calcareous marine sediments sites were selected because of their long time record and because of the variable $CaCO_3$ content of the sediments, ranging from 29.5 to 87 wt % for samples selected from ODP 846B and ranging from 19.0 to 85.9 wt % for samples selected from ODP 704A. The Pacific Ocean samples were dated between 0.09 and 17.70 Myr, and Atlantic samples were dated between 1 and 3.44 Myr [*Ciesielski et al.*, 1988; *Mayer et al.*, 1992]. ODP 846B is a subequatorial drill hole located at 90°W off the coast of Ecuador, south of the Galapagos islands. ODP 704A is a drill core located in the South Atlantic, 45°S 10°E, southwest off the coast of South Africa.

2.2.1.2. Magnesium Chemical Separation

[7] The Mg separation for Fe-Mn nodules requires two columns. A first anionic column was used to separate Fe, Mg, Mn and Ca from the monovalent cations (column 1: 2 ml of AG1-X8 resin, 200–400 mesh), and a second cationic column was used, with a resin of higher cross linkage (i.e., AG50-X12), to separate Mg from the other remaining cations, especially from Ca (column 2: 1.25 ml of AG50W-X12 resin, 200–400 mesh). The 0.9 ml remaining after the HF attack was diluted up to 10 ml with HCl 2% and an aliquot of 100 to 200 μl of each sample was dried, redissolved in 0.3 ml of concentrated HCl and loaded on column 1. Elution was done with 7 ml concentrated HCl (i.e., 2 × 3 ml + 1 ml). All the acids were distilled prior to use and columns were HF cleaned as described in a previous study by *Chang et al.* [2003]. After evaporation and dissolution in 0.3 ml of 1N HCl, each sample was loaded on column 2. We discarded the first 10 ml of HCl 1N elution volume and kept the magnesium that falls with the next 5 × 5 ml HCl 1N elutions. We then evaporated these 25 ml. The final dry residue is dissolved in 2 ml 0.05N HCl and ready for multicollector (MC)-ICP-MS plasma 54 measurements. For the samples, the recovery of Mg after column chemistry was 95% within the analytical uncertainty of the Mg concentration measurements (i.e., 5%). To validate the procedure, the standard DSM3 was run through this column chemistry and the δ^{26}Mg for DSM3 varies between 0.04 and 0.27‰ compared to its reported literature data (0‰ by definition [*Galy et al.*, 2003]). This yield-induced isotope shift is less than or similar to our analytical reproducibility (i.e., ±0.36‰, 2σ on a sample). We did not run any carbonate standard like other recent studies [*Wombacher et al.*, 2009] but validated our procedure using the regular DSM3 standard solution

Table 1. Instrumental Operating Conditions on the Inductively Coupled Plasma–Mass Spectrometer Plasma 54 of ENS Lyon and Signal Measurement Parameters for the Mg Isotope Analysis

Parameter	Description
rf power	1350 W
Plasma gas flow rate	17L/min
Interface cones	nickel wide-angle skimmer cone
Acceleration voltage	6 kV
Ion lens setting	optimized for max. intensity
Instrument resolution	300
Mass analyzer pressure	2×10^{-9} mbar
Detector	9 Faraday collectors
Nebulizer	microconcentric
Spray chamber temp.	75°C
Desolvator temp.	160°C
Swep gas (argon)	2.6L/min (optimized daily)
Sample uptake rate	40μl/min
^{24}Mg sensitivity	7 V/0.25 ppm
Sampling time	two repetitions of 300 s
Background time	two repetitions of 10 s

[*Galy et al.*, 2002]. To our knowledge, no Fe-Mn standard exists, so to have a suitable comparable matrix for the nodules was difficult. To test the procedure on a matrix other than carbonate, San Carlos olivine was measured after column chemistry, with an average δ^{26}Mg = +3.42 ± 0.06‰ (normalized to NBS980, for two replicates of the entire Mg chemical separation procedure) which is within the analytical uncertainty compared to its average laser ablation reported in the literature data, +2.99 ± 0.25‰ (also normalized to NBS980 [*Pearson et al.*, 2006]).

2.2.2. Calcareous Sediments

2.2.2.1. Sample Preparation and Attack

[8] Calcareous sediment samples consisted of cylindrical 2 cm long cores of marine sediments. They were washed three times with ultrapure water. Although clay input is low relative to biogenic fluxes at site 846 (Pacific [*Mayer et al.*, 1992]) and not observed at site 704 (Atlantic [*Ciesielski et al.*, 1988]), the finest particles were discarded by gravitational separation (i.e., shaking, letting settle one minute and discarding the overlying topmost water). After drying in a Teflon beaker and crushing in an agate mortar, 10–15 mg of powder was weighed and leached with 2 ml of 0.1N HNO_3 to dissolve the carbonate fraction of the sediment. After dissolution, the residue was separated by centrifuging. The supernatant liquid was evaporated to dryness and dissolved in 1 ml of 2N HCl.

2.2.2.2. Magnesium Chemical Separation

[9] The chemical separation of Mg on the supernatant was done using a slightly modified procedure after *Chang et al.* [2003, 2004]. We used the same second column as in the case of nodules (i.e., 1.25 ml of 200–400 mesh resin) but the first column was also an AG50W-X12 cationic column (0.78 ml of 200–400 mesh resin), to efficiently separate Mg, Na and Ca. To avoid potential $^{12}C^{14}N$ mass interference, HCl was used for the elution acid instead of HNO_3. The sample was loaded and eluted on the first column in HCl 2N in order to separate (Na + Mg) from Ca. After drying the recovered 9 ml (i.e., 3 × 3 ml) of the eluted solution, and subsequently redissolving it in 0.3 ml of HCl 1N, the sample was then loaded on the second column to separate Na from Mg. The first 2 × 5 ml of elution with HCl 1N were discarded and the following 25 ml of elution with HCl 1N were kept, dried and retaken in 2 ml of HCl 0.05N for ICP-MS analysis. During this procedure, it has been described that a partial elution with a recovery of 90% Mg would induce an isotopic shift smaller than our analytical uncertainty (0.13‰ [*Chang et al.*, 2003] compared to our analytical uncertainty of ±0.36‰ for a sample in this study). Once Mg is purified, the final dry residue was redissolved in 2 ml 0.05 N HCl before isotope measurements on the MC-ICP-MS plasma 54.

2.3. Mass Spectrometry

[10] The instrumental setting and measurement procedure is identical for manganese nodules and carbonate samples. All purified Mg solutions are introduced into the MC-ICP-MS (Plasma 54 at ENS Lyon, France) via an ARIDUS desolvating nebulizer. This MC-ICP-MS is a magnetic sector instrument with variable dispersion ion optics and a fixed array of 9 Faraday collectors. The operating conditions adopted for the mass spectrometer are summarized in Table 1. The settings are mostly conventional [e.g., *Galy et al.*, 2001] except for the wide-angle nickel skimmer cone, which increases the signal, and therefore reduces the sample load in the machine. The Plasma 54 MC-ICP-MS produces Mg peaks with flattops at a working mass resolution power of 300, as required for precise isotope ratio measurements [*Galy et al.*, 2001]. The three Mg isotopes are positioned in the multiple collector on the 9 available Faraday cups, for simultaneous measurements as follows: ^{26}Mg in the one before the last cup on the high-mass side of the

Table 2. Location, Sampling Depth, Tungsten and Magnesium Concentrations, and Magnesium Isotope Composition of Ferromanganese Nodules[a]

Sample	Latitude	Longitude	Depth (m)	W (ppm)	Mg (ppm)	δ^{26}Mg Per Mil	δ^{26}Mg $\pm2\sigma$[b]	δ^{25}Mg Per Mil	δ^{25}Mg $\pm2\sigma$[b]
Indian Ocean									
384C	35°51S	36°46E	5450	6.9	8706	+0.56	0.01	+0.27	0.01
CP7912	32°40S	50°45E	4300	9.4	7427	+0.69	0.18	+0.33	0.13
CP7916	24°22S	58°21E	5000	5.6	8127	−0.02	0.49	−0.06	0.29
AET7611	24°05S	59°55E	4425	89.5	8949	−1.94	0.53	−1.18	0.29
DR7506	44°00S	59°57E	4840	41.2	7138	−1.62	0.52	−0.98	0.36
AET7610	31°21S	61°55E	4245	53.2	9167	−1.43	0.01	−0.90	0.01
DR7704	23°22S	62°23E	4400	13.7	5777	+0.65	0.19	+0.22	0.05
DR7507	47°16S	62°45E	3910	22.8	10764	−1.10	0.53	−0.66	0.31
AET7718	16°49S	74°38E	4430	13.5	9893	+0.05	0.28	−0.03	0.03
DR8605	58°02S	77°01E	2600	139.2	7212	−2.94	0.46	−1.72	0.20
CP8130	13°35S	77°03E	5270	148.5	14596	−2.69	0.44	−1.53	0.30
DR8607	55°18S	77°28E	2510	88.4	7674	−1.11	0.06	−0.75	0.06
CP8123	11°51S	78°39E	5060	69.3	12442	−1.65	0.19	−0.96	0.26
EPC49–26	51°22S	95°05E	3585	31.5	9314	−0.60	0.61	−0.31	0.24
Pacific Ocean									
E14–12	52°01S	159°53W	2853	34.4	8546	−0.94	0.05	−0.68	0.05
E20–13 (average)	60°20S	137°50W	4289	34.3	8450	−1.40	0.36	−0.85	0.16
E20–13[c]						−1.57	0.09	−0.91	0.04
E20–13[c]						−1.43	0.06	−0.87	0.06
E20–13[c]						−1.21	0.13	−0.76	0.07
E25–12	49°59S	104°53W	3877	61.4	9947	−0.86	0.07	−0.60	0.06
MP43-B	12°03N	165°00E	2125–1529	nd	294	−1.89	0.24	−1.16	0.39
TUNESO6WT25D	20°27N	155°55E	2300–2100	nd	532	−1.60	0.27	−0.85	0.18
DODO 9–2D	18°18N	161°46W	3111	nd	330	−0.54	0.01	−0.24	0.14
MERO2P50	13°52S	150°35W	3695	nd	437	−1.27	nd	−0.64	nd
South America									
E05–07B	59°02S	67°18W	3475	22.6	8670	−0.17	0.16	−0.15	0.10
Atlantic Ocean									
RC15-D5	48°28S	55°14W	2500	83.6	7959	−0.71	0.04	−0.53	0.05
T1678–117	44°01S	33°05W	5201	29.4	12073	−0.93	0.06	−0.44	0.05
V29-D12	22°27S	07°33E	3265	86.4	8236	−0.97	0.14	−0.52	0.10
Agulhas Basin									
RC14-D1	37°52S	26°41E	2900	42.7	13955	−1.13	0.06	−0.64	0.06

[a]Tungsten concentrations were performed on an Inductively Coupled Plasma–Mass Spectrometer, model X7 with a typical analytical uncertainty of 5%. nd, not determined.
[b]Each sample is run three times. For each sample, the reported 2-sigma error is two times the standard deviation of the three measurements. As a result, reported 2-sigma errors are variable depending on the stability of the machine.
[c]Triplicate.

multiple collector; ^{25}Mg in the axial cup; and ^{24}Mg in the one before the last cup on the low-mass side of the multiple collector.

[11] For the measurement procedure, we use a standard sample bracketing technique, with the magnesium isotopic standard DSM3 [*Galy et al.*, 2003]. With this protocol, standard and sample isotope values are measured four and three times, respectively. To avoid cross contamination between the sample and the standard, we washed the analytical instrumentation system and the cones with 0.05N HCl for 5–10 min between analyses. Results are expressed as a per mil deviation from the isotopic composition of the standard:

$$\delta^{26}Mg = \left(\frac{\left({}^{26}Mg/{}^{24}Mg \right)_{sample}}{\left({}^{26}Mg/{}^{24}Mg \right)_{DSM3}} - 1 \right) \times 1000$$

[12] The δ^{26}Mg external reproducibility on the standard solution DSM3 is ±0.20‰ (2σ, n = 60, determined over several sessions). The reproduc-

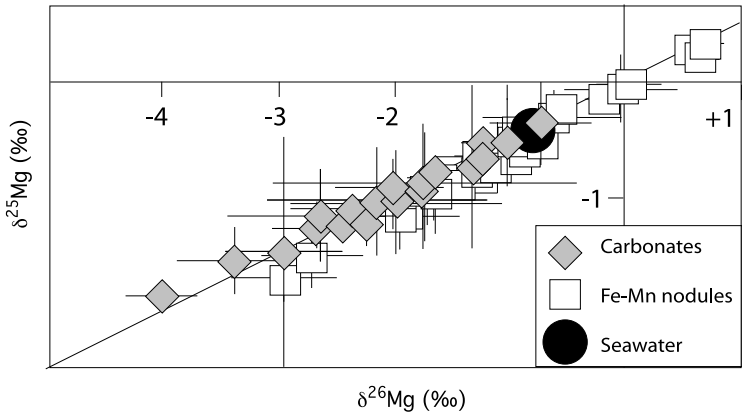

Figure 2. Values of δ^{25}Mg versus δ^{26}Mg for Fe-Mn nodules (open squares) and carbonate samples (gray diamonds). All samples are on the terrestrial fractionation line (black line). Although there is a lot of overlap, Fe-Mn nodules have, on average, higher δ^{26}Mg than the average carbonate sample. The filled circle represents the composition of seawater (δ^{26}Mg = −0.80 ± 0.04‰ for the Atlantic Ocean [*Young and Galy*, 2004]). Note that only the calcareous samples for which [Ca]/[Mg] is <0.5 were kept for Mg isotopic analysis to avoid potential double-charged ^{48}Ca interference on ^{24}Mg [*Galy et al.*, 2001]. Although the value of 0.5 could already induce matrix-related mass bias, no relationship between internal errors and Ca/Mg of the measurement solution was reported, and all samples and standards plot on the terrestrial fractionation line.

Table 3. Age, $CaCO_3$, Mg Concentrations, and Magnesium Isotope Compositions of the Calcareous Sediments From ODP704A and ODP846B[a]

Meters Below Sea Level[b]	Age[b] (Ma)	$CaCO_3$[b] (wt %)	δ^{26}Mg Per Mil	δ^{26}Mg 2σ	δ^{25}Mg Per Mil	δ^{25}Mg 2σ	Mg (ppm)
		ODP114, 704 A, 46°53S, 7°25E: Atlantic					
45.77	0.9998	44.1	−1.97	0.92	−1.07	0.44	374.1 ± 1.2
66.83	1.3336	21.1	−1.73	0.62	−0.96	0.51	384.4 ± 2.3
66.83[c]			−1.95	0.60	−1.14	0.29	
98.28	1.8392	44.2	−2.42	0.53	−1.28	0.10	430.9 ± 2.1
133.38	2.1481	50.9	−2.22	0.12	−1.27	0.18	239.6 ± 3.3
142.24	2.2323	31.7	−1.97	0.06	−0.97	0.03	242.8 ± 3.5
145.24	2.2589	78.3	−1.23	0.04	−0.68	0.01	701.1 ± 0.9
150.24	2.3032	19.0	−1.00	0.23	−0.53	0.38	330.1 ± 1.3
151.74	2.3165	80.4	−2.34	0.55	−1.14	0.16	413.3 ± 3.9
172.25	2.7428	55.4	−1.21	0.19	−0.54	0.12	699.5 ± 0.7
173.75	2.7983	85.9	−1.31	0.13	−0.76	0.72	361.0 ± 3.7
175.25	2.8538	76.7	−0.71	0.45	−0.37	0.36	923.4 ± 1.2
177.36	2.9093	80.5	−2.94	0.50	−1.50	1.01	407.4 ± 3.9
187.37	3.4380	75.6	−1.97	0.40	−1.07	0.23	541.5 ± 0.7
		ODP138, 846 B, 3°06S, 90°49W: Pacific					
3.75	0.0891	29.5	−1.73	1.31	−0.89	0.50	1791.3 ± 0.5
93.25	2.7317	37.1	−2.66	0.38	−1.29	0.17	352.7 ± 0.2
134.25	3.9508	59.3	−2.62	0.80	−1.18	0.40	835.8 ± 1.2
168.42	4.8691	78.2	−4.00	0.31	−1.88	0.11	480.1 ± 0.7
322.75	11.2580	72.2	−1.63	0.09	−0.80	0.11	909.6 ± 1.0
335.45	11.9672	66.0	−1.99	0.50	−0.94	0.25	484.5 ± 0.3
386.28	15.5965	87.0	−3.36	0.51	−1.58	0.29	557.1 ± 0.5
411.15	17.2192	75.6	−2.13	0.96	−1.05	0.48	1020.5 ± 0.8
419.00	17.7032	61.9	−1.73	0.06	−0.92	0.03	2178.9 ± 0.3

[a] $CaCO_3$ in weight percent are also reported.
[b] From ODP preliminary initial reports [*Ciesielski et al.*, 1988; *Mayer et al.*, 1992].
[c] Duplicates.

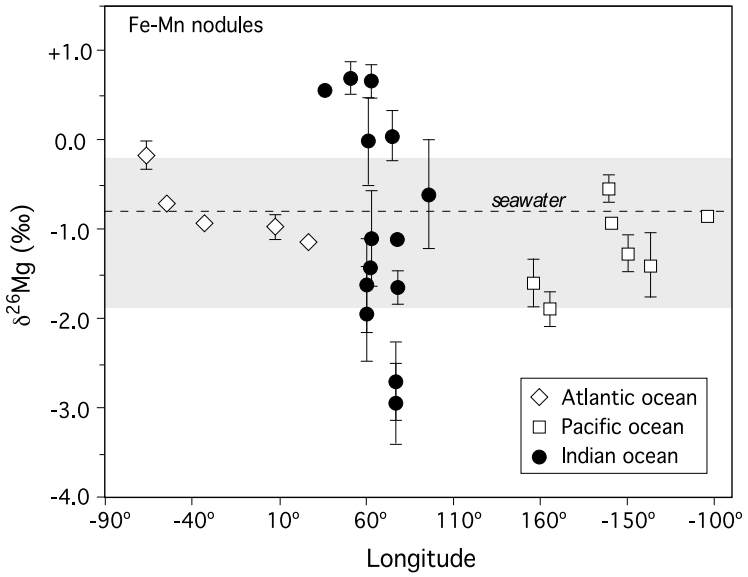

Figure 3. Values of δ^{26}Mg of the Fe-Mn nodules as a function of the longitude of the sampling site. The three ocean basins display resolvable differences in magnesium isotope values. The Pacific samples in particular have δ^{26}Mg between −1.89 ± 0.24 and −0.54 ± 0.01‰, both lower and higher values than the δ^{26}Mg value of the Atlantic water (−0.80 ± 0.04‰, dashed line [*Young and Galy*, 2004]). Both Atlantic (open diamonds) and Pacific (open squares) nodules have restricted δ^{26}Mg ranging from −1.89 ± 0.24 to −0.17 ± 0.16‰ (shaded area). Nodules from the Indian Ocean (filled circles) have the largest δ^{26}Mg variations, ranging from −2.94 ± 0.46 to +0.69 ± 0.18‰. Samples are all in the Southern Hemisphere, mostly clustered around the Rodriguez triple junction. They cover an area between 95°05E and 36°46E longitude and between 11°51S and 58°02S latitude.

ibility of the whole chemical procedure on the δ^{26}Mg of a single sample is ±0.36‰ (2σ, n = 3 (Table 2)). All samples and standards plot on the terrestrial fractionation line (Figure 2). Each sample is run three times and the reported 2-sigma errors are two times the standard deviation of the three measurements (Tables 2 and 3). As a result, the reported 2-sigma errors are variable depending on the stability of the machine.

3. Results

[13] Results are reported in Tables 2 and 3 and are plotted in Figure 3 as a function of their sampling longitude for the ferromanganese nodules.

3.1. Calcareous Sediments

[14] The values of δ^{26}Mg in the carbonate fraction of the marine sediments range from −4.00 ± 0.31‰ to −0.71 ± 0.45‰ with several peaks in the depth profile (Table 3).

3.1.1. Site ODP114 704A

[15] In terms of carbonate chemistry there are differences among oceans. The cored sediments from site 704A consist of varying admixtures of two end-member components: (1) calcareous oozes and chalks consisting of foraminifers and calcareous nannofossils and (2) siliceous oozes composed of diatoms with minor radiolarians and silicoflagellates [*Ciesielski et al.*, 1988].

3.1.2. Site ODP138 846B

[16] Clay input at site 846B is low relative to biogenic fluxes. The dominant sediment component at site 846 alternates between biogenic silica (mostly diatoms) and calcium carbonates (mostly nannofossils). The lower ≈39 m of the sediment column is dominated by nannofossils and has been compacted to chalk.

[17] Our δ^{26}Mg measurements of the carbonate fraction of the sediments are in agreement with previous studies on carbonate rocks, foraminifera tests and corals that have reported δ^{26}Mg values consistently lower than that of seawater [*Galy et al.*, 2001, 2002; *Chang et al.*, 2003, 2004; *Pogge von Strandmann*, 2008; *Hippler et al.*, 2009]. The formation of coral aragonite approximates to inorganic precipitation from a seawater reservoir in terms of Mg [*Chang et al.*, 2004]. In contrast, the δ^{26}Mg of foraminifera calcite is systematically

Table 4. Transition Element Composition of the Ferromanganese Nodules

Sample	Mn (%)	Fe (%)	Cu (%)	Co (%)	Ni (%)	Zn (ppm)	Cr (ppm)
			Indian Ocean				
384C	14.20	8.80	0.200	0.120	0.460	579	21
CP7912[a]	15.64	13.51	0.142	0.281	0.413	574	8
DR7301[a]	15.60	16.99	0.063	1.215	0.250	640	<5
DR7301 duplicate	14.81	16.79	0.053	1.121	0.223	701	3
CP7916[a]	13.71	10.81	0.194	0.188	0.332	456	63
AET7611[a]	11.69	16.21	0.062	0.325	0.123	415	28
DR7506[a]	16.07	13.86	0.196	0.149	0.596	804	20
AET7610[a]	14.30	11.74	0.205	0.197	0.388	603	7
DR7704[a]	11.75	15.83	0.086	0.301	0.165	461	19
DR7507[a]	15.97	7.20	0.270	0.101	0.909	1195	42
AET7718[a]	17.30	12.39	0.349	0.214	0.615	698	<5
DR8605[a]	21.10	8.85	0.044	1.055	0.508	716	<5
CP8130[a]	26.40	5.20	1.248	0.108	1.258	1425	15
DR8607[a]	16.42	16.09	0.030	0.544	0.224	618	6
DR8607 duplicate	15.25	14.19	0.029	0.473	0.181	633	3
CP8123	20.54	8.04	0.628	0.134	0.935	944	<5
EPC49–26	20.98	13.74	0.163	0.177	0.555	770	n.d.
			Pacific Ocean				
E14–12	14.46	12.65	0.172	0.144	0.422	912	8
E20–13[a]	22.50	7.96	0.432	0.051	0.500	890	n.d.
E25–12	16.27	15.12	0.227	0.115	0.405	743	5
MP43-B	7.03	32.43	0.050	1.473	0.767	1076	17
TUNES O6WT 25D	8.95	34.16	0.085	0.980	0.540	918	39
DODO 9–2D	14.76	38.25	0.082	0.766	0.465	1078	16
MERO2P50	8.09	35.94	0.292	0.910	0.493	990	10
			South America				
E05–07B	10.56	13.48	0.102	0.185	0.146	531	10
			Atlantic Ocean				
RC15-D5	15.63	15.82	0.027	0.389	0.145	553	3
T1678–117[a]	19.95	6.03	0.223	0.019	0.400	1210	n.d.
V29-D12	15.26	15.78	0.025	0.466	0.166	482	5
			Agulhas Basin				
RC14-D1	21.87	3.85	0.676	0.112	0.904	1214	8

[a]Data from *Albarède et al.* [1997].

lower than that of seawater and presents significant variation between and within species (−4.34 to −5.11‰ and, e.g., −5.06 to −5.31‰ for G. sacculifer, respectively [*Pogge von Strandmann*, 2008]). In addition, it is reported that calcite has systematically a δ^{26}Mg approximately 2‰ lower than that of dolomite [e.g., *Young and Galy*, 2004].

3.2. Ferromanganese Nodules

[18] The geographic distribution of nodules with their δ^{26}Mg isotope values is given in Figure 3. Samples can be described following the ocean basins. The Pacific nodules have δ^{26}Mg between −1.89 ± 0.24 and −0.54 ± 0.01‰ (Table 2). These samples have both lower and higher values than the δ^{26}Mg value of the Atlantic water (−0.80 ± 0.04‰ [*Young and Galy*, 2004]). The Atlantic and Pacific nodules show less variation around the oceanic δ^{26}Mg value of −0.80 ± 0.04‰ (Table 2).

[19] In a triangular plot of Fe, Mn, and (Cu+Zn+Ni) × 10 [*Dymond et al.*, 1984] for the present samples (Table 4 and Figure 4), two of the three end-members explain most of the variability of the Indian Ocean and Atlantic Ocean nodules. Nodules' mineralogy is classically todorokite and vernadite [e.g., *Halbach et al.*, 1981; *Uspenskaya et al.*, 1987]. The main difference between the two mineralogies is that vernadite contains Co and is considered as hydrogenous in origin, whereas todorokite has no or low Co and it has a diagenetic origin. A previous study brings an additional layer of complexity demonstrating that todorokite can form from vernadite [*Bodeï et al.*, 2007]. δ^{26}Mg of the nodules does not correlate with Co concentration, which suggests that the mineralogy of

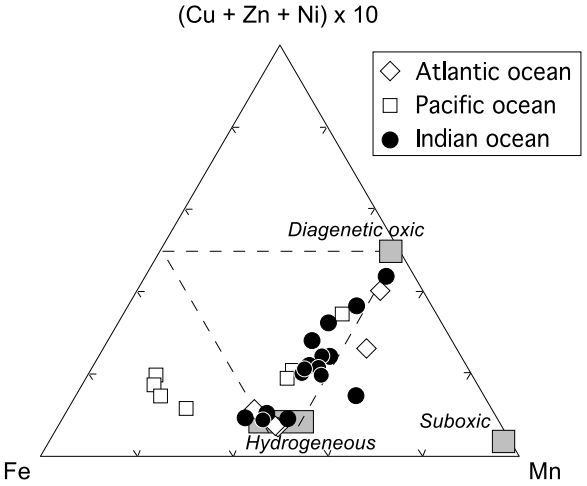

Figure 4. Triangular plot of Fe, Mn, and (Cu+Zn+Ni) × 10 for the Fe-Mn nodules, following the plot scheme of *Dymond et al.* [1984]. The diagenetic oxic and hydrogenous end-members explain most of the variability of the Indian Ocean (filled circles) and Atlantic Ocean (open diamonds) nodules. Five samples, the most enriched in (Cu+Zn+Ni) × 10 (>30), are under oxic diagenetic control. Four samples from the Pacific (open squares) are enriched in Fe.

the nodule is less likely the main control of the observed magnesium isotope variations.

4. Discussion

[20] In the following discussion it is assumed that Mg isotope compositions of open ocean water are homogenous because of the long residence time of magnesium in the ocean.

4.1. Influence of Diagenesis on the Magnesium Isotope Compositions of Fe-Mn Nodules

[21] Both todorokite and vernadite minerals occur as original phases in a nodule (early diagenetic: todorokite; hydrogenetic: vernadite) but the abundance of todorokite increases after the deposition due to two types of processes: (1) an in situ transformation of vernadite to todorokite [*Bodeï et al.*, 2007], which is conditioned by the presence of magnesium in seawater which plays a key role in converting the phyllomanganate precursor (vernadite) into todorokite [*Bodeï et al.*, 2007], and (2) diagenesis in the sediment, triggered for example by a change of oxidation conditions, with the remobilization from sediments, lateral transport and diagenetic enrichment of both Mn and Fe in the concretions which favors the mineralogical form of todorokite [e.g., *Marcus et al.*, 2004]. Another indicator of early diagenesis in Fe-Mn nodules is W concentration. The concentrations of W in Pacific ferromanganese nodules are 34 to 61 ppm (Figure 5). The W concentrations in the other oceans overlap with this range but are much more variable, from 7 to 149 ppm for the Indian Ocean nodules and between 23 and 86 ppm for the Atlantic nodules (Figure 5). The Indian Ocean samples display a negative correlation between their δ^{26}Mg and W (Figure 5). This is another line of evidence showing that the lower δ^{26}Mg values, at least for the Fe-Mn nodules of the Indian Ocean, are related to diagenesis; that is, they are the most enriched in W.

4.2. Magnesium Isotope Compositions of Calcareous Sediments

4.2.1. Mineralogical Control

[22] It has been shown that the magnitude of magnesium isotope fractionation during precipitation from seawater is smaller for mineral phases such as aragonite ($\delta^{26}Mg_{sw} - \delta^{26}Mg_{aragonite} = 0.94‰$) than in the case of calcite ($\delta^{26}Mg_{sw} -$

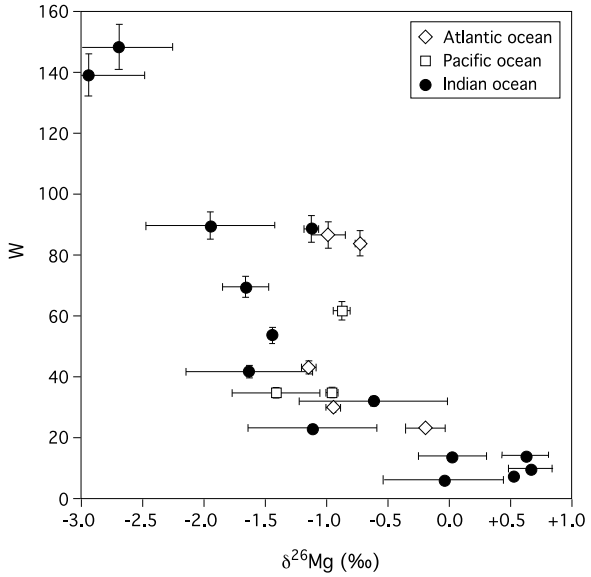

Figure 5. Tungsten as a function of δ^{26}Mg in oceanic Fe-Mn nodules. WO_4^{2-} concentration in the oceans is constant from the surface to the bottom [*Sohrin et al.*, 1987], but it is concentrated in oceanic sediments, and they can therefore act as a source of W for the Mn oxides [*Kishida et al.*, 2004]. Elevated W is therefore considered as an indicator of increase diagenesis. The negative correlation of W with δ^{26}Mg suggests that the calcareous sediments and/or alteration products end-members have a δ^{26}Mg < −3‰.

$\delta^{26}Mg_{calcite}$ = 2.7‰; inorganic calcite [*Galy et al.*, 2002]; high-Mg calcite corals [*Wombacher et al.*, 2006; *Pogge von Strandmann*, 2008; *Kisakurek et al.*, 2009]). Therefore the range of variation in δ^{26}Mg from Pacific and Atlantic carbonates could be explained by difference in carbonate precipitation between calcite and aragonite, but this assumption is hard to confirm without any information on the mineralogy of the carbonates.

4.2.2. Influence of Diagenesis and Biology

[23] The $\delta^{26}Mg^{carb}_{DSM3}$ values of modern carbonate fraction of marine sediments vary between −4.00 and −0.71‰. A recent study has determined that several benthic and planktonic foraminifera have identical $^{26}Mg/^{24}Mg$ ratios, with an average δ^{26}Mg = −4.72‰ [*Pogge von Strandmann*, 2008]. Three species of foraminifera differ from the δ^{26}Mg average by no more than ±0.4‰. According to this author, the insusceptibility of δ^{26}Mg values to external parameters (T, Mg/Ca) makes Mg isotopes ideally suited to constraining past marine δ^{26}Mg variations. Other type of micro-organisms with a different metabolism (e.g., corals) can have different δ^{26}Mg. Therefore the δ^{26}Mg variations that we observe are interpreted as a mixture of different tests of micro-organisms, with each type carrying the expression of Mg isotope fractionation between seawater and its carbonate test. The δ^{26}Mg values of the carbonate fraction of the sediments are all $<\delta^{26}Mg_{seawater}$, which means that marine micro-organisms fractionate seawater Mg isotopes by keeping preferentially ^{24}Mg and they can therefore be considered as a light Mg isotope reservoir. This is in agreement with what is observed on a variety of other skeletal carbonates [*Hippler et al.*, 2009]. Overall the variations observed are a due to the variety of micro-organisms with different $CaCO_3$ polymorphs, and to a certain extent to the diagenesis of carbonates in sediments. When pH of sediment pore waters changes, some carbonates become unstable and dissolve. In other pH conditions different carbonate phases will recrystallize and we expect magnesium isotopes to fractionate similarly to what happens during carbonate precipitation, leading to a global light magnesium isotope enrichment in the newly precipitated carbonate.

5. Conclusion

[24] We report Mg isotope composition of Fe-Mn nodules from the Pacific, Atlantic and Indian oceans and δ^{26}Mg of marine carbonates from the Pacific and Atlantic oceans.

[25] Pacific and Atlantic nodules show small variations in δ^{26}Mg, within ±1‰ from the δ^{26}Mg of seawater ($\delta^{26}Mg^{seawater}_{DSM3} = -0.80 \pm 0.04$‰ [e.g., *Young and Galy*, 2004]), whereas Indian Ocean nodules have δ^{26}Mg ranging from −2.94 ± 0.46 to +0.69 ± 0.18‰. These δ^{26}Mg variations correlate negatively with W concentrations and are interpreted as a first-order indicator of early oxic diagenesis.

[26] Marine carbonates from the Pacific and from the Atlantic have δ^{26}Mg varying from −4.00 ± 0.31 to −1.63 ± 0.09‰ and from −2.94 ± 0.5 to −0.71 ± 0.45‰, respectively. δ^{26}Mg variations that we observe are interpreted as due to a mixture between different test of micro-organisms and also to the influence of diagenesis.

Acknowledgments

[27] We are grateful to W. Abouchami for providing four samples from the Pacific. We thank C. Douchet who diligently always made everything available in the clean room and P. Telouk for his technical assistance. E.R.-K. thanks F. Wombacher for his critical comments on an earlier version of the manuscript. Constructive reviews by Seth John, Edward Tipper, and Vincent Salters (Editor) were greatly appreciated and substantially improved the manuscript. This research used samples and data provided by the Ocean Drilling Program (ODP). ODP is sponsored by the U.S. National Science Foundation (NSF) and participating countries under management of Joint Oceanographic Institutions (JOI), Inc.

References

Abouchami, W., and S. L. Goldstein (1995), A lead isotopic study of circum-Antarctic manganese nodules, *Geochim. Cosmochim. Acta*, *59*(9), 1809–1820, doi:10.1016/0016-7037(95)00084-D.

Albarède, F., S. L. Goldstein, and D. Dautel (1997), The neodymium isotopic composition of manganese nodules from the Southern and Indian oceans, the global oceanic neodymium budget, and their bearing on deep ocean circulation, *Geochim. Cosmochim. Acta*, *61*(6), 1277–1291, doi:10.1016/S0016-7037(96)00404-8.

Albarède, F., A. Simonetti, J. D. Vervoort, J. Blichert-Toft, and W. Abouchami (1998), A Hf-Nd isotopic correlation in ferromanganese nodules, *Geophys. Res. Lett.*, *20*, 3895–3898.

Berner, E. K., and R. A. Berner (1996), *Global Environment: Water, Air, and Geochemical Cycles*, Prentice Hall, Upper Saddle River, N. J.

Bodeï, S., A. Manceau, N. Geoffroy, A. Baronnet, and M. Buatiera (2007), Formation of todorokite from vernadite in Ni-rich hemipelagic sediments, *Geochim. Cosmochim. Acta*, *71*, 5698–5716.

Brenot, A., et al. (2008), Magnesium isotope systematics of the lithologically varied Moselle river basin, France, *Geochim. Cosmochim. Acta*, *72*, 5070–5089, doi:10.1016/j.gca.2008.07.027.

Broecker, W. S., and T. H. Peng (1982), *Tracers in the Sea*, 690 pp., Lamont-Doherty Geol. Obs., Palisades, N. Y.

Chang, V. T.-C., A. Makishima, N. S. Belshaw, and R. K. O'Nions (2003), Purification of Mg from low-Mg biogenic carbonates from isotope ratio determination using multiple collector ICP-MS, *J. Anal. At. Spectrom.*, *18*, 296–301, doi:10.1039/b210977h.

Chang, V. T.-C., R. J. P. Williams, A. Makishima, N. S. Belshaw, and R. K. O'Nions (2004), Mg and Ca isotope fractionation during $CaCO_3$ biomineralisation, *Biochem. Biophys. Res. Commun.*, *323*, 79–85, doi:10.1016/j.bbrc.2004.08.053.

Ciesielski, P. F., et al. (1988), *Proceedings of the Ocean Drilling Program, Initial Reports*, vol. 114, 815 pp., Ocean Drill. Program, College Station, Tex.

de Villiers, S., and B. K. Nelson (1999), Detection of low-temperature hydrothermal fluxes by seawater Mg and Ca anomalies, *Science*, *285*, 721–723, doi:10.1126/science.285.5428.721.

de Villiers, S., J. A. D. Dickson, and R. M. Ellam (2005), The composition of the continental river weathering flux deduced from seawater Mg isotopes, *Chem. Geol.*, *216*, 133–142, doi:10.1016/j.chemgeo.2004.11.010.

Dymond, J., B. Lyle, B. Finney, D. Z. Piper, K. Murphy, R. Conard, and N. Pisias (1984), Ferromanganese nodules from MANOP sites H, S, and R—Control of mineralogical and chemical composition by multiple accretionary processes, *Geochim. Cosmochim. Acta*, *48*, 931–949, doi:10.1016/0016-7037(84)90186-8.

Edmond, J. M., C. Measures, R. E. McDuff, L. H. Chan, R. Collier, B. Grant, L. I. Gordon, and J. B. Corliss (1979), Ridge crest hydrothermal activity and the balances of the major and minor elements in the ocean: The Galapagos data, *Earth Planet. Sci. Lett.*, *46*, 1–18, doi:10.1016/0012-821X(79)90061-X.

Galy, A., N. S. Belshaw, L. Halicz, and R. K. O'Nions (2001), High-precision measurement of magnesium isotopes by multiple-collector inductively coupled plasma mass spectrometry, *Int. J. Mass Spectrom.*, *208*(1–3), 89–98, doi:10.1016/S1387-3806(01)00380-3.

Galy, A., M. Bar-Matthews, L. Halicz, and R. K. O'Nions (2002), Mg isotopic composition of carbonate: Insight from speleothem formation, *Earth Planet. Sci. Lett.*, *201*, 105–115, doi:10.1016/S0012-821X(02)00675-1.

Galy, A., et al. (2003), Magnesium isotope heterogeneity of the isotopic standard SRM980 and new reference materials for magnesium-isotope-ratio measurements, *J. Anal. At. Spectrom.*, *18*, 1352–1356, doi:10.1039/b309273a.

Halbach, P., C. Scherhag, U. Hebisch, and V. Marchig (1981), Geochemical and mineralogical control of different genetic types of deep-sea nodules from the Pacific Ocean, *Miner. Deposita*, *16*, 59–64, doi:10.1007/BF00206455.

Hart, S. R., and H. Staudigel (1982), The control of alkalies and uranium in seawater by ocean crust alteration, *Earth Planet. Sci. Lett.*, *58*(2), 202–212, doi:10.1016/0012-821X(82)90194-7.

Hippler, D., D. Buhl, R. Witbaard, D. K. Richter, and A. Immenhauser (2009), Towards a better understanding of magnesium-isotope ratios from marine skeletal carbonates, *Geochim. Cosmochim. Acta*, *73*, 6134–6146, doi:10.1016/j.gca.2009.07.031.

Kisakurek, B., A. Niedermayr, M. N. Muller, I. Taubner, A. Eisenhauer, M. Dietzel, D. Buhl, J. Fietzke, and J. Erez (2009), Magnesium isotope fractionation in inorganic and biogenic calcite, *Geochim. Cosmochim. Acta*, *73*(13), suppl. 1, A663.

Kishida, K., Y. Sohrin, K. Okamura, and J. Ishibashi (2004), Tungsten enriched in submarine hydrothermal fluids, *Earth Planet. Sci. Lett.*, *222*, 819–827, doi:10.1016/j.epsl.2004.03.034.

Mackenzie, F. T., and R. M. Garrels (1966), Chemical mass balance between rivers and oceans, *Am. J. Sci.*, *264*, 507–525.

Marcus, M. A., A. Manceau, and M. Kersten (2004), Mn, Fe, Zn and As speciation in a fast-growing ferromanganese marine nodule, *Geochim. Cosmochim. Acta*, *68*, 3125–3136.

Mayer, L., et al. (1992), *Proceedings of the Ocean Drilling Program, Initial Reports*, vol. 138, 674 pp., Ocean Drill. Program, College Station, Tex.

Mottl, M. J., and G. Wheat (1994), Hydrothermal circulation through mid-ocean ridge flanks: Fluxes of heat and magnesium, *Geochim. Cosmochim. Acta*, *58*, 2225–2237, doi:10.1016/0016-7037(94)90007-8.

Pearson, N. J., W. L. Griffin, O. Alard, and S. Y. O'Reilly (2006), The isotopic composition of magnesium in mantle olivine: Records of depletion and metasomatism, *Chem. Geol.*, *226*, 115–133, doi:10.1016/j.chemgeo.2005.09.029.

Pogge von Strandmann, P. A. E. (2008), Precise magnesium isotope measurements in core top planktic and benthic foraminifera, *Geochem. Geophys. Geosyst.*, *9*, Q12015, doi:10.1029/2008GC002209.

Pogge von Strandmann, P. A. E., K. W. Burton, R. H. James, P. van Calsteren, S. R. Gislason, and B. Sigfusson (2008), The influence of weathering processes on riverine magnesium isotopes in a basaltic terrain, *Earth Planet. Sci. Lett.*, *276*, 187–197, doi:10.1016/j.epsl.2008.09.020.

Sohrin, Y., M. Matsui, and E. Nakayama (1987), Tungsten in North Pacific waters, *Mar. Chem.*, *22*, 95–103, doi:10.1016/0304-4203(87)90051-X.

Spencer, R. J., and L. A. Hardie (1990), Control of seawater composition by mixing of river waters and mid-ocean ridge hydrothermal brines, in *Fluid-Mineral Interactions: A Tribute to H. P. Eugster*, edited by R. J. Spencer and I. M. Chou, *Spec. Publ. Geochem. Soc.*, *19*, 409–419.

Tipper, E. T., A. Galy, and M. J. Bickle (2006a), Riverine evidence for a fractionated reservoir of Ca and Mg on the continents: Implications for the oceanic Ca cycle, *Earth Planet. Sci. Lett.*, *247*, 267–279, doi:10.1016/j.epsl.2006.04.033.

Tipper, E. T., A. Galy, J. Gaillardet, M. J. Bickle, H. Elderfield, and E. A. Carder (2006b), The magnesium isotope budget of the modern ocean: Constraints from riverine magnesium isotope ratios, *Earth Planet. Sci. Lett.*, *250*, 241–253, doi:10.1016/j.epsl.2006.07.037.

Tipper, E. T., A. Galy, and M. J. Bickle (2008), Calcium and magnesium isotope systematics in rivers draining the Himalaya-Tibetan-Plateau region: Lithological or fractionation control, *Geochim. Cosmochim. Acta*, *72*, 1057–1075.

Uspenskaya, T. Y., A. I. Gorshkov, and A. V. Sivtsov (1987), Mineralogy and internal structure of Fe–Mn nodules from the Clarion–Clipperton fracture zone, *Int. Geol. Rev.*, *29*, 363–371, doi:10.1080/00206818709466153.

Vlastelic, I., W. Abouchami, S. J. G. Galer, and A. W. Hofmann (2001), Geographic control on Pb isotope distribution and sources in Indian Ocean Fe-Mn deposits, *Geochim. Cosmochim. Acta*, *65*(23), 4303–4319, doi:10.1016/S0016-7037(01)00713-X.

Wilkinson, B. H., and T. J. Algeo (1989), Sedimentary carbonate record of calcium-magnesium cycling, *Am. J. Sci.*, *289*, 1158–1194.

Wombacher, F., A. Eisenhauer, F. Böhm, N. Gussone, H. Kinkel, J. Lezius, S. Noé, M. Regenberg, and A. Rüggeberg (2006), Magnesium stable isotope compositions in biogenic $CaCO_3$, *Geophys. Res. Abstr.*, *8*, 06353.

Wombacher, F., A. Eisenhauer, A. Heuser, and S. Weyer (2009), Separation of Mg, Ca and Fe from geological reference materials for stable isotope ratio analyses by MC-ICP-MS and double-spike TIMS, *J. Anal. At. Spectrom.*, *24*, 627–636, doi:10.1039/b820154d.

Young, E. D., and A. Galy (2004), The isotope geochemistry and cosmochemistry of magnesium, in *Geochemistry of Non-Traditional Stable Isotopes*, *Rev. in Mineral. and Geochem.*, vol. 55, edited by C. M. Johnson, B. L. Beard, and F. Albarède, pp. 197–230, Mineral. Soc. of Am., Washington, D. C.